Applied Physics Letters

Intracellular simulated biophoton stimulation and transsynaptic signal transmission

Cite as: Appl. Phys. Lett. **121**, 203701 (2022); https://doi.org/10.1063/5.0128956
Submitted: 02 October 2022 • Accepted: 28 October 2022 • Published Online: 14 November 2022

Na Liu, Zhuo Wang and Jiapei Dai

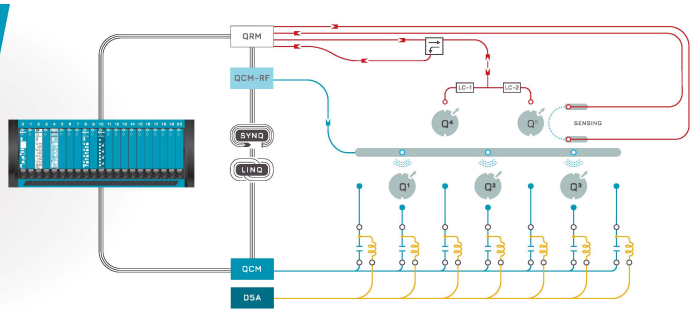

Applied Physics Letters ARTICLE scitation.org/journal/apl

Intracellular simulated biophoton stimulation and transsynaptic signal transmission

Cite as: Appl. Phys. Lett. **121**, 203701 (2022); doi: 10.1063/5.0128956
Submitted: 2 October 2022 · Accepted: 28 October 2022 ·
Published Online: 14 November 2022

Na Liu,[1,2] Zhuo Wang,[1,2] and Jiapei Dai[1,2,a)]

AFFILIATIONS

[1]Wuhan Institute for Neuroscience and Neuroengineering, South-Central Minzu University, Wuhan 430074, China
[2]The College of Life Sciences, South-Central Minzu University, Wuhan 430074, China

[a)]**Author to whom correspondence should be addressed:** jdai@mail.scuec.edu.cn. **Tel.:** +86-27-67840917

ABSTRACT

The traditional theory holds that the information transmission between nerve cells includes electrical and chemical transmission; however, these known functional features do face some difficulties to explain the fast and efficient information processing and cognitive processes in the brain due to the existing functional limitations of neuronal networks, such as the dendritic and axonal propagation delays as well as the chemical synaptic transmission time delay that have been debated for a long time. We generated three kinds of ultraweak lasers, called as simulated biophotons, with different spectra and intensities to implement intracellular stimulation in a single nerve cell of the hippocampal areas in mouse brain slices combined with intracellular membrane potential recording and biophoton imaging techniques. We found that the simulated biophoton stimulation can lead to transsynaptic biophotonic activities and transmission in the ipsilateral and contralateral projection circuits in the hippocampus. The activity and transmission characteristics were related to the spectra and intensities of the simulated biophotons but not to the levels of membrane potentials before stimulation. These findings present specific characteristics of neural biophoton signal transmission, which may be involved in the mechanisms of processing, encoding, and storage of neural signals.

The information transmission between nerve cells includes electrical and chemical transmission. Electrical transmission mainly mediates the conduction of action potentials on axons and across electrical synapses directly, whereas chemical transmission mediates synaptic information transmission by means of the action mechanisms of neurotransmitters and their receptors.[1] However, these known structural and functional features fail to explain the fast and efficient information processing and cognitive processes in the brain, in which some have believed to be impossible due to the existing structural and functional limitations of neuronal networks, such as the dendritic and axonal propagation delays as well as the chemical synaptic transmission time delay that have been debated for a long time.[2–9] Although different assumptions including the communication-through-coherence (CTC) hypothesis[6–9] and the ephaptic coupling hypothesis[10,11] have been put forward to explain these problems; however, so far, there is no clear consensus. The latest studies have demonstrated that biophotons, also called ultraweak photon emission (UPE), may play a role in neural information transmission and processing, which is different from the electrical transmission along the nerve fibers and the chemical transmission across the chemical synapses, and may involve photon quantum brain mechanism.[12–15] Although the theoretical analysis have also showed that the biophotonic transmission along the nerve fibers is feasible, and the structural features of nerve fibers, such as polar microtubule assembly, myelin sheath, and the node of Ranvier, provide a basis for the biophotonic transmission;[16–18] however, it is still unknown what are the characteristics of biophotonic activities and transmission in the neural circuits.

We constructed a systemic technique (Fig. 1) by integrating intracellular membrane potential recording, single nerve cell intracellular ultraweak laser (simulated biophoton) stimulation, and biophoton imaging technology. By setting the initial light intensity (voltage or current dependence) of three lasers (red: 650 nm, green: 532 nm, and blue: 405 nm) and using a combination of neutral density filters on an optic attenuator, the ultraweak lasers at high, medium, and low intensities were obtained and regarded as simulated biophotons. A laser was used as a stimulus light source because biophotons have similar laser characteristics.[19] The low, medium, and high levels of simulated biophotons radiated from the tip of the optic fiber within the microglass tube were evaluated with the ultraweak biophoton imaging system (UBIS), and the relative gray values (RGVs) were approximately

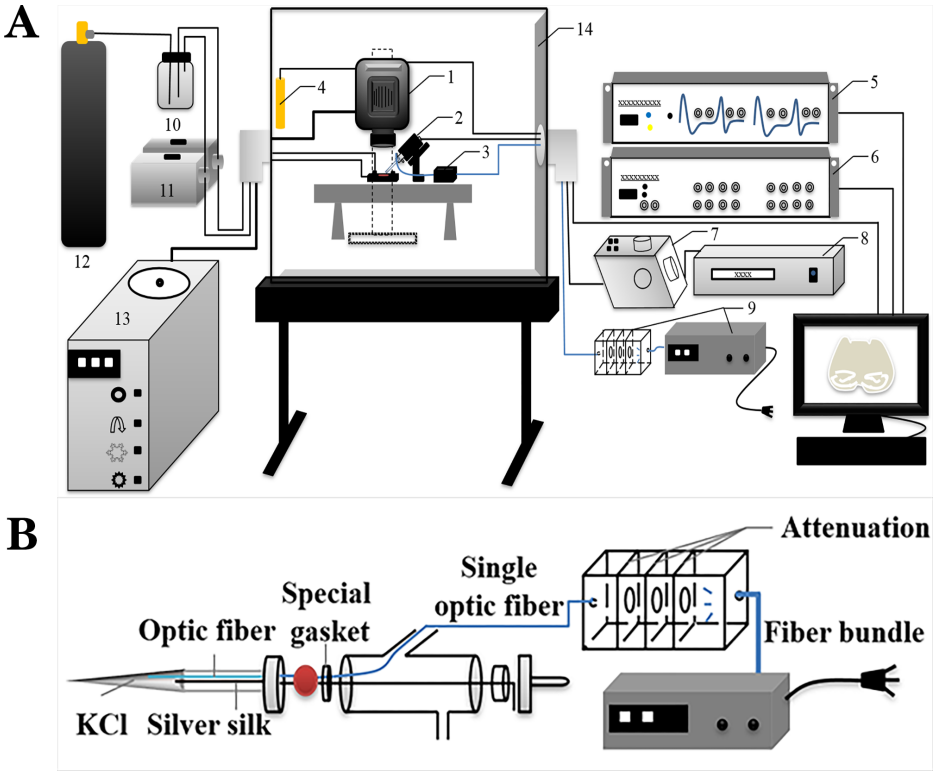

FIG. 1. Technological diagram of membrane potential recording, simulated biophoton stimulation, and biophoton imaging in single nerve cells. (a) Schematic diagram of integration devices, including the ultraweak biophoton imaging system (UBIS), the simulated biophoton generator, and the brain slice perfusion chamber. 1—EMCCD; 2—the holder of the micromanipulator for the micro-glass tube containing the electrode and the single multimode optic fiber; 4—copper bar; 5—current and voltage clamp amplifier; 6—digital converter; 7—micromanipulator; 8—micromanipulator controller; 9—laser light source, optic attenuator, and neutral density filters (dimmers); 10—perfusion bottle; 11—micropump; 12—gas bottle; 13—circulating water cooler; and 14—dark box. (b) The improved part of the micro-glass tube probe and the simulated biophoton generator, ensuring that the recording electrode and optic fiber for ultraweak light stimulation can easily be placed into the micro-glass tube.

900, 1800, and 3600, respectively [Figs. 2(A) and 2(B)], of which the high intensity was approximately 12 times the average intensity level of biophoton emissions in a mouse brain slice induced by 50 mM glutamate[12] [Fig. 2(C) and Table S1] since biophoton intensity can be considerably higher inside cells than outside.[20] Two types of simulated biophoton stimulation paradigms (paradigms I and II) in a single nerve cell were carried out 5 min after the collection of the membrane potential signal (synchronous continuous imaging) [Figs. 2(D) and 2(E)]. Paradigm I was implemented with the stimulations at a high intensity level of simulated green biophoton [Fig. 2(D)], while paradigm II was used to stimulate the recording nerve cells with the simulated red, green, and blue biophotons at the three different intensities [Fig. 2(E)], but each recording nerve cell was only stimulated with one of the three types of simulated biophotons. In this study, we carried out intraneuronal simulated biophoton stimulation of single nerve cells in mouse hippocampal slices[21–24] (see the details in Material and methods of the supplementary material) and observed transsynaptic signal transmission in the intra- and extra-hippocampal projection circuits.

We obtained 164 effective data from the hippocampal slices, of which 93 and 71 data were from the simulated biophoton stimulation paradigms I (Table S2) and II (Table S3), respectively. Through data analysis, it was found that, under the condition of paradigm I, the proportion of obvious biophotonic activity and transmission in both the ipsilateral and contralateral hippocampus (both side) caused by simulated biophoton stimulation in a single nerve cell of the hippocampus and other areas was 45.16% (42/93) [Figs. S1(a)–S1(C) and Table S2], while the proportion of ipsilateral biophotonic activity and transmission was 50.54% (47/93) [Figs. S1(d)–S1(f) and Table S2]. There were also 16 recorded cells that were deviated from the hippocampus (17.2%, 16/93) and located in the dorsal thalamus and cortex [Fig. S1(g) and Table S2]. We also found that a small proportion of nerve cells (4.3%, 4/93) whose membrane potentials could be recorded showed only minor or no ipsilateral or contralateral biophotonic activity and transmission in the projection areas of the hippocampus after simulated biophoton stimulation [Fig. S1(h) and Table S2].

Table S2 shows the detailed distribution areas and the intensity of biophotonic activities after stimulation of a single nerve cell in the dentate gyrus (DG), CA3 and CA1 areas, and other areas deviated from the hippocampus. The main activity areas after stimulation of a single nerve cell in DG area were the ipsilateral CA3, CA2, CA1, and dorsal thalamus (lateral geniculate nucleus), and partially the contralateral hippocampal areas [Figs. S1(a) and S1(d)]. While the biophotonic activities and transmission were observed in the ipsilateral CA1, the thalamus, and even the hypothalamus after stimulation of a single nerve cell in the CA3 area [Fig. S1(b)]. In addition, some cells resulted in biophotonic activities and transmission in the ipsilateral sensory and motor cortexes [Figs. S1(b) and S1(e)]. For the stimulation of a single nerve cell in the CA1 area, the main areas of biophotonic activity and transmission were noticed in the bilateral or unilateral DG, CA1, thalamus, and retrosplenial agranular/granular cortex (RSA/RSG) [Figs. S1(c) and S1(f)]. The biophotonic activities and transmission after stimulation of a single nerve cell in the dorsal part of thalamus were mainly observed in the ventral part of thalamus, the ipsilateral hippocampal areas, the dorsal part of hypothalamus, and the primary somatosensory cortex [Fig. S1(g)].

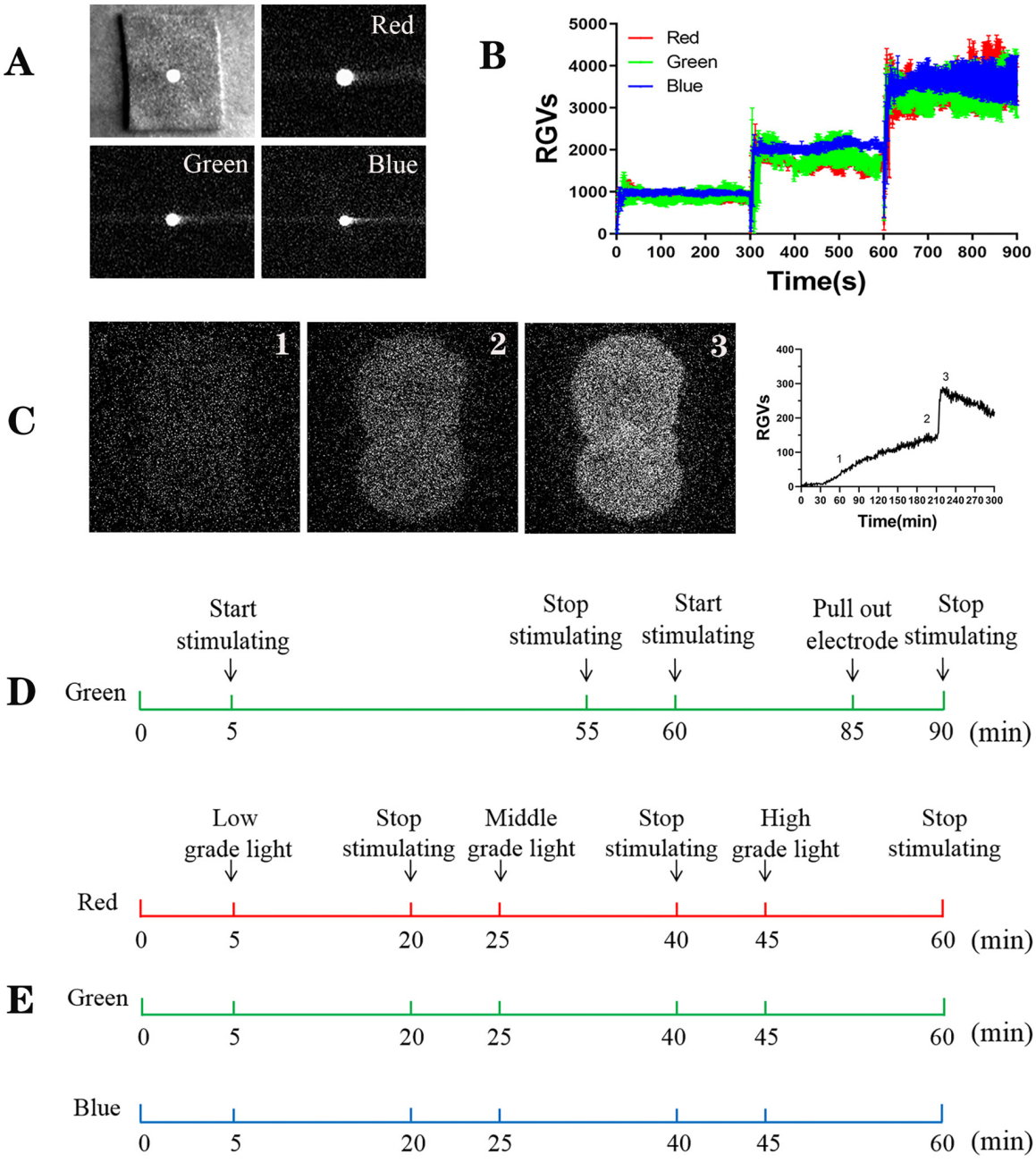

FIG. 2. Simulated biophoton assessment and stimulation paradigm. (a) Photon acquisition images obtained from three color ultraweak lasers (simulated biophotons). The figures from left to right are positioning photographs, and red, green, and blue imaging images, respectively; (b) evaluation of the intensities (RGVs) of the red, green, and blue simulated biophotons at low, medium, and high levels of stimulation; (c) imaging biophotonic activities after the application of 50 mM glutamate in a mouse coronal brain slice [c(1)–c(3)] and the dynamic change in biophotonic activities demonstrated by relative gray values [c(right panel)] during the initiation and maintenance periods; (d) Simulated green biophoton stimulation paradigm (paradigm I) at the high grade of stimulation; and (e) the simulated biophoton stimulation paradigm (paradigm II) for different intensities of red, green, and blue (from top to bottom). The exposure time is 1 s/frame.

Under the condition of paradigm I, we analyzed the dynamic change in the biophotonic activity and transmission in the bilateral or unilateral hippocampus induced by simulated biophoton stimulation of a single nerve cell. For the bilateral biophotonic activity and transmission, the target areas of the ipsilateral and contralateral projection circuits in the hippocampal area showed a certain range of biophotonic activities that reached a maximum amplitude immediately and then maintained a relatively stable level [Fig. 3(A)]. After stopping

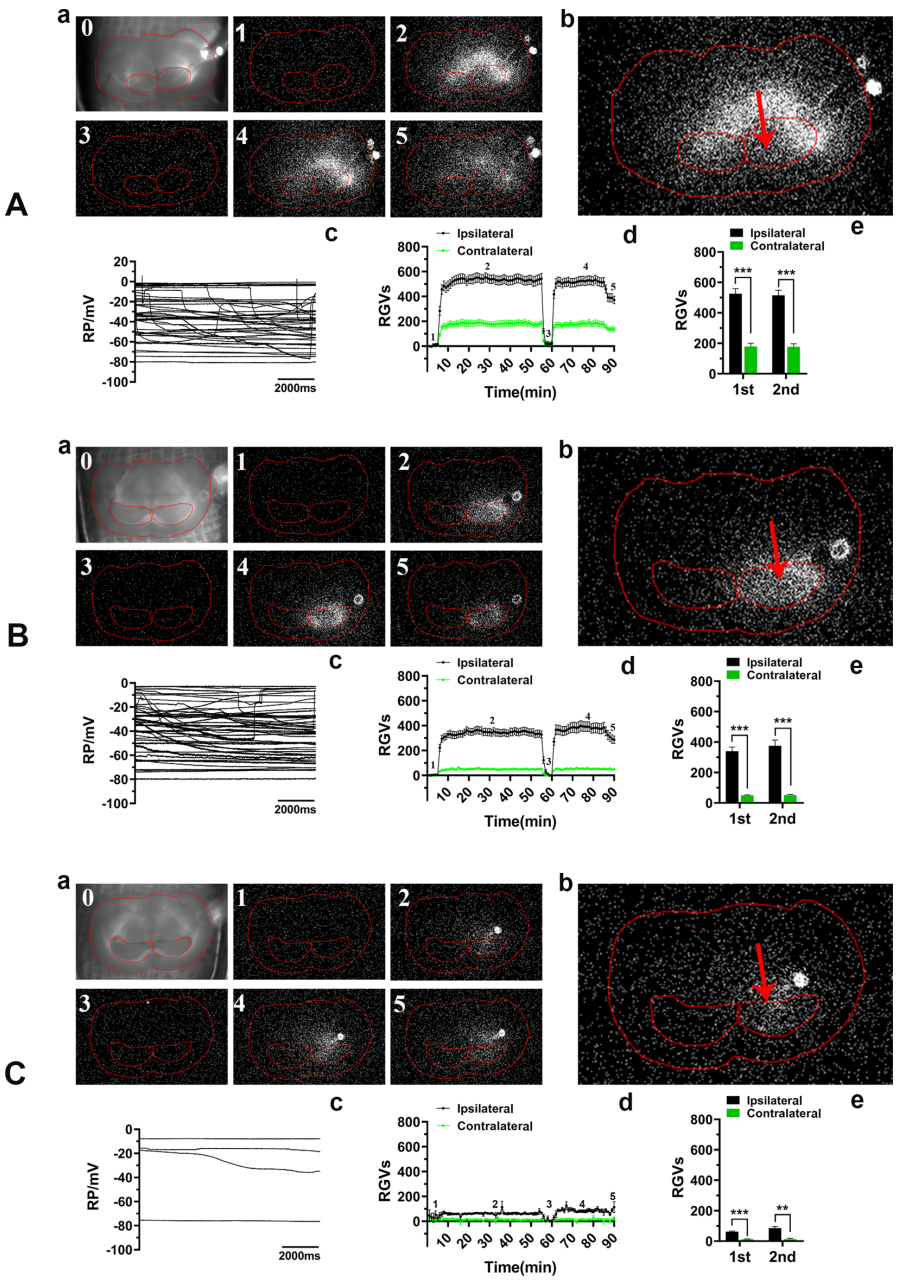

FIG. 3. Characteristic changes in biophotonic activities in bilateral and unilateral hippocampal circuits after paradigm I-stimulated biophoton stimulation. (A) The characteristic changes in biophotonic activities and transmission in bilateral hippocampal circuits in a representative of the brain slice, showing a regular photo (numeral 0) and five imaging images [A(a)]. The start, maintenance, stop, and restart of stimulations as well as the move of the stimulation from the intracellular to the extracellular sites were indicated by the numbers 1–5. The edge of the brain slice is marked by a large irregular red circle in the regular slice photo (numeral 0) and the two small red ones indicate the ROI for quantitative evaluation of the intensities of biophotonic activities in the ipsilateral and contralateral hippocampus, and the same was applied to the other five photon imaging images [A(a)]. An enlarged image corresponding to an image in A(a) [number 2, the same case as in Fig. S1(A)], and the red arrow indicates the tip of the micro-glass tube inserted into a nerve cell [A(b)]. The changes in the membrane potential of 42 nerve cells recorded before simulated biophoton stimulation [A(c)]. The average change curves of RGVs in ipsilateral (black line) and contralateral (green line) target areas of the hippocampus ($n = 42$) and the numerals 1–5 correspond to the five photon imaging images in A(d). The comparison of the difference (RGVs) in the ipsilateral (black line) and contralateral (green line) target areas of the hippocampus between the first (5–55 min) and second stimulation (61–85 min) [A(e)]; (B) characteristic changes in the biophtonic activities and transmission in unilateral hippocampal circuits. The information for all figures is almost the same as in (A) with the exception of the number of nerve cells tested ($n = 47$); (C) characteristic changes in the intensities of biophtonic activities in the ipsilateral and contralateral hippocampal areas in four nerve cells with minor or no obvious biophotonic activities. The information for all figures is almost the same as in (A) with the exception of the number of nerve cells tested ($n = 4$). Data show mean ± s.e.m. $^{**}P < 0.01$, $^{***}P < 0.001$.

the stimulation at 55 min, the biophotonic activities decreased rapidly close to the background level, and the decline process did not show a phenomenon of exponential attenuation, such as an induced luminescence [Fig. 3(A)]. The response characteristics caused by repeat stimulation beginning at 60 min were consistent with those during the first stimulation [Fig. 3(A)], and the average amplitude of increase was not significantly different between the first and second stimulations [Fig. 3(A), $P > 0.05$, $n = 42$]. When the simulated biophoton stimulation was maintained, but the tip of the micro-glass tube was removed from the recording cell at 85 min, the biophotonic activities in the neural circuits showed a rapid decline, and then maintained a very low level of emissions [Fig. 3(A)]. In addition, the intensity of biophotonic activities in the target area of the ipsilateral hippocampus was significantly higher than that in the target area of the contralateral hippocampus [Fig. 3(A), $P < 0.001$, $n = 42$].

In the case of only ipsilateral biophotonic activities and transmission after simulated biophoton stimulation, the biophotonic activities increased rapidly after the first stimulation but took a relatively long time to reach the maximum amplitude and then remained stable [Fig. 3(B)]. In addition, the biophotonic activity pattern was consistent with that of the bilateral activities after stopping and repeating the stimulation at 55 min and 60 min, respectively, or moving the stimulation from the intracellular to the extracellular sites at 85 min [Fig. 3(B)]. We also compared the intensities of the biophotonic activities in four nerve cells without obvious ipsilateral or contralateral biophotonic activities after simulated biophoton stimulation and found that the intensities were very weak although there was a statistical difference between the stimulated side and the non- stimulated side [Fig. 3(C)]. In addition, the similar dynamic changes in biophotonic activities and transmission in bilateral and unilateral hippocampus were noticed if the analysis was emphasized on the stimulation of a single nerve cell in the DG area (Fig. S2).

We further explored the effects of the change in the simulated biophoton intensities and spectra on the biophotonic activities and transmission under the condition of paradigm II (Table S3). There was no significant difference in the membrane potential levels including the instantaneous membrane potential (IMP) and the average membrane potential (AMP) under the different stimulations [Fig. 4(A)]. We found that with the increase in simulated biophoton stimulation intensities, the biophotonic activities, and transmission were also increased in the hippocampal neural circuits [Fig. 4(B)]. The intensities of the ipsilateral biophotonic activities caused by the simulated red and green biophoton stimulations at the low and medium levels of intensities were not different, but their effects were more obvious than those caused by the simulated blue biophoton stimulation [Figs. 4(C) and 4(D)]. In addition, the effect of the simulated red biophoton stimulation at a high intensity was more obvious than that of the simulated blue and green biophoton stimulations [Fig. 4(C)], and the activity area was relatively wider [Fig. 4(B)]. Under medium and high stimulation intensities, the intensities and area of biophotonic activities in the contralateral area of the hippocampus caused by simulated red biophoton stimulation were more evident than those caused by simulated green and blue biophoton stimulation [Figs. 4(C) and 4(D)].

We also analyzed the relationship between the membrane potential state of nerve cells and the biophotonic activity and transmission pattern in the hippocampal neural circuits caused by simulated green biophoton stimulations under the condition of paradigm I. It was found that the distribution range of AMP was almost same no matter the biophotonic activities and transmission occurred in the bilateral (-2 and -80 mV) or unilateral (-3 and -80 mV) hippocampal neural circuits (Fig. S3 and Table S2). In addition, there was no correlation between the intensities of biophotonic activities and AMPs (Fig. S4).

In this study, we demonstrated that simulated biophoton stimulation in single nerve cells could lead to transsynaptic biophotonic activities and transmission in hippocampal neural circuits, which could support our previous indirect experimental observations [12,14,15] and other theoretical model speculations.[16–18] Additionally, the technology developed in this study may provide an important method for further exploring the relationship between biophotons and brain functions, for example, whether an *in vivo* simulated biophoton stimulation simulation in a single cell in a specific brain region of animal could control the specific functional activities, such as limb movement.

The characteristics of biophotonic activities and transmission in the hippocampal neural circuit caused by simulated biophoton stimulation in a single nerve cell are highly consistent with the anatomical projection circuits of the hippocampal areas;[21–24] however, simulated biophoton stimulation of a single nerve cell could induce activities in a relatively wide range of neural networks, suggesting that biophotonic activities and transmission in neural circuits may reflect a highly cooperative transsynaptic network mechanism. However, whether such a mechanism involves the principle of a "photon quantum brain" proposed previously needs to be further verified.[13,14] For example, how the traditional principles of entanglement, coherence, and superposition in quantum mechanics could work in biophotonic activities and transmission in neural circuits needs to be further verified.

Unexpectedly, we found that the simulated biophoton stimulation of some nerve cells with relatively small membrane potential could also lead to obvious biophotonic activities and transmission, suggesting that the biophotonic activity and transmission induced by the simulated biophoton stimulation in a single nerve cell may have no relationship with its membrane potential state. It has been traditionally believed that the generation and conduction of action potentials are directly related to the membrane potential; however, previous studies demonstrated that it is very sparse or silent for most of the neurons in the hippocampus, neocortex, and cerebellum under the appropriate behavioral conditions.[25–27]

Interestingly, in this study, we found that the patterns of biophotonic activities and transmission in the hippocampal neural circuit caused by different simulated biophoton stimulations were related to their spectra and intensities. Under the same intensity, red light stimulation resulted in stronger and wider effects of activities and transmission than green and blue light stimulation. It is unknown whether such effects are related to the biological characteristics of the targeted nerve cells. Our previous research found that the biophotons emitted from brain slices of various species induced by glutamate presented spectral redshift from low to high species, and the red laser wavelength (650 nm) used in this study was similar to the average wavelength of the biophoton (647 nm) in mouse brain slices induced by glutamate.[28] In addition, blue light stimulation could not effectively induce biophotonic activity and transmission in the contralateral neural circuit of the mouse hippocampus. These findings suggest that simulated red biophotons may be more conducive to transmission and are more

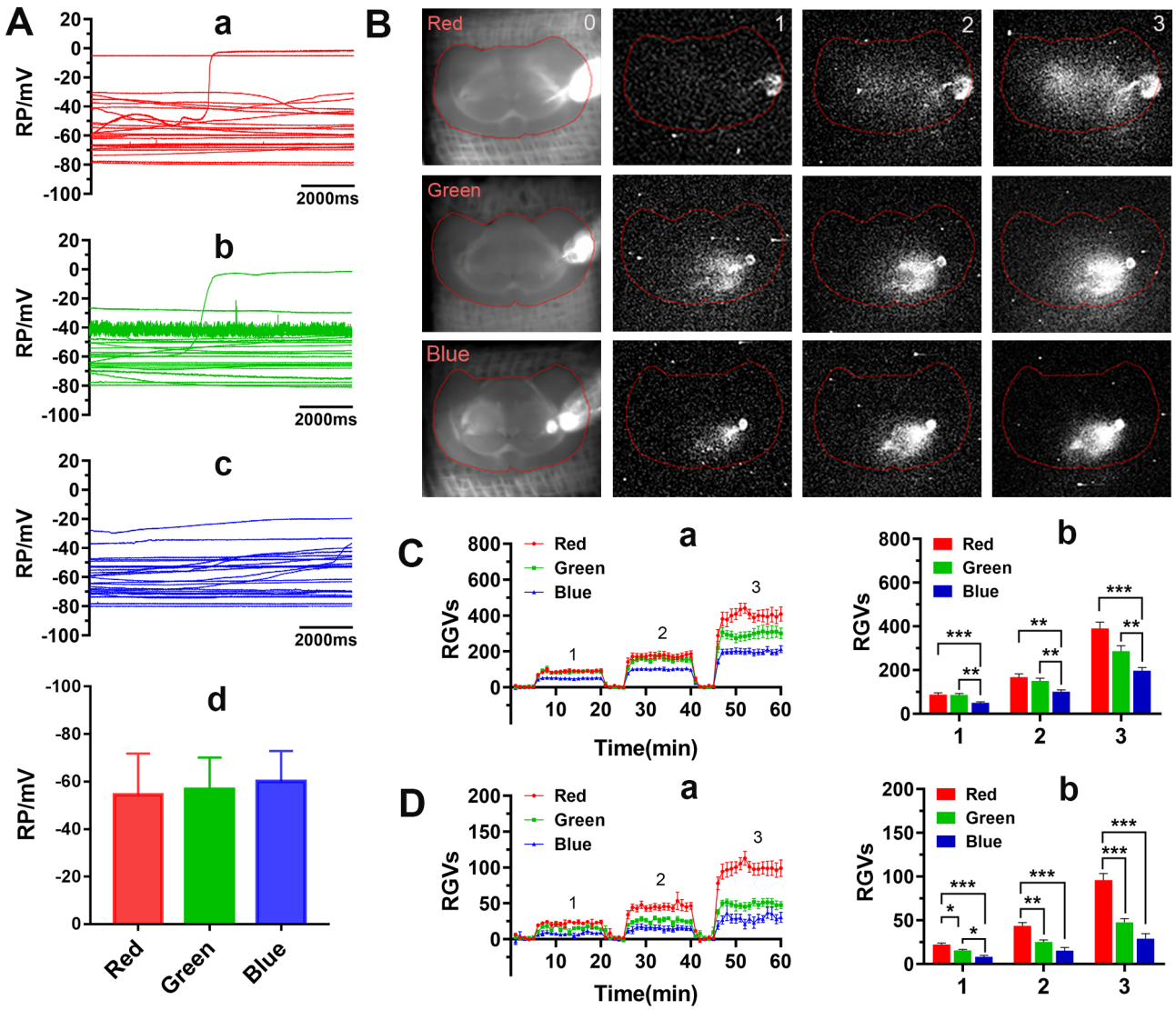

FIG. 4. Characteristic changes in biophotonic activities related to the intensities and spectra of the simulated biophotons. (A) The change curve of each nerve cell membrane potential in 10 s recorded from 24, 24, and 23 cells for the red [A(a)], green [A(b)], and blue [A(c)] simulated biophoton stimulation and biophoton imaging, respectively. There was no significant difference in the AMP levels under the different stimulations [A(d)]; (B) Three representative brain slices (regular photo, number 0) and their photon imaging images after intracellular red, green, and blue simulated biophoton stimulation (paradigm II) in the DG area of the hippocampus (irregular red circle). Images (numbers 1–3) are the merged images of 1–20, 21–40, and 41–60 min, respectively, showing the biophotonic activities at the low, medium, and high levels of stimulation and presenting more obvious biophotonic activities not only in intensities but also in the width after red simulated biophoton stimulation than after green and blue simulated biophoton stimulation; (C) and (D) The dynamic change in biophotonic activities in the contralateral [C(a)] and ipsilateral [D(a)] hippocampus after low (1–20 min), medium (21–40 min), and high (41–60 min) levels of red (red line), green (green line), and blue (blue line) simulated biophoton stimulation. Statistical analysis of biophotonic activities in the contralateral [C(b)] and ipsilateral [D(b)] hippocampus between the different colors at the three intensities. n = 24, 24, and 23 for red, green, and blue, respectively. Data show mean ± s.e.m. $^{*}P < 0.05$, $^{**}P < 0.01$, and $^{***}P < 0.001$.

suitable and effective for the processing of neural information in mouse neural circuits than simulated blue biophotons.

In conclusion, our research results show that simulated biophoton stimulation in single nerve cells in mouse hippocampal slices could lead to transsynaptic biophotonic activities, which not only opens a perspective for clarifying the information transmission and processing mechanism of the brain but also provides ideas for the development of quantum computing and artificial intelligence because non-delayed propagation of information in neural circuits could be realized via biophotons through quantum effects of entanglement, coherence, and superposition.

See the supplementary material for the complete electronic structure of detailed methods and supplementary figures and tables.

This work was supported by the Wuhan frontier project for applied foundational research (No. 2019020701011452), the innovation team fund of National Ethnic Affairs Commission (No. MZR20002), and the research funds of South-Central Minzu University (No. CZP 18003).

AUTHOR DECLARATIONS

Conflict of Interest

The authors have no conflicts to disclose.

Ethics Approval

Ethics approval for experiments reported in the submitted manuscript on animal or human subjects was granted. The study protocol was approved by the Committee on the Ethics of Experimental Animals and Biomedicine of South-Central Minzu University (No: 2017-SCUEC-AEC-007).

Author Contributions

Na Liu: Data curation (equal); Formal analysis (equal); Funding acquisition (supporting); Investigation (equal); Methodology (equal); Project administration (supporting); Resources (equal); Writing – original draft (equal). **Zhuo Wang:** Funding acquisition (supporting); Investigation (supporting); Methodology (supporting). **Jiapei Dai:** Conceptualization (lead); Data curation (equal); Formal analysis (equal); Funding acquisition (lead); Investigation (equal); Methodology (equal); Project administration (lead); Resources (lead); Supervision (lead); Validation (lead); Writing – original draft (equal); Writing – review & editing (lead).

DATA AVAILABILITY

The data that support the findings of this study are available from the corresponding author upon reasonable request.

REFERENCES

[1]P. Dale, J. A. George, and F. David, *Neuroscience*, 3rd ed. (Sinauer Associates, Inc., Sunderland, Massachusetts, USA, 2004), pp. 31–126.
[2]H. Hogendoorn and A. N. Burkitt, "Predictive coding with neural transmission delays: A real-time temporal alignment hypothesis," eNeuro **6**, ENEURO.0412–18 (2019).
[3]W. Bialek, "Physical limits to sensation and perception," Annu. Rev. Biophys. Biophys. Chem. **16**, 455–478 (1987).
[4]W. Bialek and S. Setayeshgar, "Physical limits to biochemical signaling," Proc. Natl. Acad. Sci. U. S. A. **102**, 10040 (2005).
[5]A. A. Faisal, L. P. J. Selen, and D. M. Wolpert, "Noise in the nervous system," Nat. Rev. Neurosci. **9**, 292–303 (2008).
[6]R. Vicente, L. L. Gollo, C. R. Mirasso, I. Fischer, and G. Pipa, "Dynamical relaying can yield zero time lag neuronal synchrony despite long conduction delays," Proc. Natl. Acad. Sci. U. S. A. **105**, 17157–17162 (2008).
[7]A. M. Bastos, J. Vezoli, and P. Fries, "Communication through coherence with inter-areal delays," Curr. Opin. Neurobiol. **31**, 173–180 (2015).
[8]P. Fries, "Rhythms for cognition: Communication through coherence," Neuron **88**, 220–235 (2015).
[9]M. Madadi Asl, A. Valizadeh, and P. A. Tass, "Dendritic and axonal propagation delays determine emergent structures of neuronal networks with plastic synapses," Sci. Rep. **7**, 1–12 (2017).
[10]C. Anastassiou, R. Perin, H. Markram, and C. Koch, "Ephaptic coupling of cortical neurons," Nat. Neurosci. **14**, 217–223 (2011).
[11]C. A. Anastassiou and C. Koch, "Ephaptic coupling to endogenous electric field activity: Why bother?," Curr. Opin. Neurobiol. **31**, 95–103 (2015).
[12]R. Tang and J. Dai, "Spatiotemporal imaging of glutamate-induced biophotonic activities and transmission in neural circuits," PLoS One **9**, e85643 (2014).
[13]R. Tang and J. Dai, "Biophoton signal transmission and processing in the brain," J. Photochem. Photobiol. B **139**, 71–75 (2014).
[14]W. Chai, Z. Han, Z. Wang, Z. Li, F. Xiao, Y. Sun, Y. Dai, R. Tang, and J. Dai, "Biophotonic activity and transmission mediated by mutual actions of neurotransmitters are involved in the origin and altered states of consciousness," Neurosci. Bull. **34**, 534–538 (2018).
[15]Z. Han, W. Chai, Z. Wang, F. Xiao, and J. Dai, "Quantum energy levels of glutamate modulate neural biophotonic signals," Photochem. Photobiol. Sci. **20**, 343–356 (2021).
[16]S. Kumar, K. Boone, J. Tuszynski, P. Barclay, and C. Simon, "Possible existence of optical communication channels in the brain," Sci. Rep. **6**, 36508 (2016).
[17]A. Zangari, D. Micheli, R. Galeazzi, and A. Tozzi, "Node of Ranvier as an array of bio-nanoantennas for infrared communication in nerve tissue," Sci. Rep. **8**, 539 (2018).
[18]M. Jibu, S. Hagan, S. R. Hameroff, K. H. Pribram, and K. Yasue, "Quantum optical coherence in cytoskeletal microtubules: Implications for brain function," Biosystems **32**, 195–209 (1994).
[19]F. A. Popp, "Properties of biophotons and their theoretical implications," Indian J. Exp. Biol. **41**, 391–402 (2003).
[20]I. Bokkon, V. Salari, J. A. Tuszynski, and I. Antal, "Estimation of the number of biophotons involved in the visual perception of a single-object image: Biophoton intensity can be considerably higher inside cells than outside," J. Photochem. Photobiol. B **100**, 160–166 (2010).
[21]L. Swanson and C. Kohler, "Anatomical evidence for direct projections from the entorhinal area to the entire cortical mantle in the rat," J. Neurosci. **6**, 3010–3023 (1986).
[22]D. G. Amaral, H. E. Scharfman, and P. Lavenex, "The dentate gyrus: Fundamental neuroanatomical organization (dentate gyrus for dummies)," Prog. Brain Res. **163**, 3–22 (2007).
[23]E. Cerasti and A. Treves, "How informative are spatial CA3 representations established by the dentate gyrus?," PLoS Comput. Biol. **6**, e1000759 (2010).
[24]I. Soltesz and A. Losonczy, "CA1 pyramidal cell diversity enabling parallel information processing in the hippocampus," Nat. Neurosci. **21**, 484–493 (2018).
[25]O. J. Ahmed and M. R. Mehta, "The hippocampal rate code: Anatomy, physiology and theory," Trends Neurosci. **32**, 329–338 (2009).
[26]A. L. Barth and J. F. Poulet, "Experimental evidence for sparse firing in the neocortex," Trends Neurosci. **35**, 345–355 (2012).
[27]J. N. Teramae, Y. Tsubo, and T. Fukai, "Optimal spike-based communication in excitable networks with strong-sparse and weak-dense links," Sci. Rep. **2**, 485 (2012).
[28]Z. Wang, N. Wang, Z. Li, F. Xiao, and J. Dai, "Human high intelligence is involved in spectral redshift of biophotonic activities in the brain," Proc. Natl. Acad. Sci. U. S. A. **113**, 8753–8758 (2016).